ACS OMEGA

http://pubs.acs.org/journal/acsodf

Article

Design and Control of Pressure-Swing Heat Integration Distillation for the Trichlorosilane Purification Process

Min Yin, Chao Hua,* Ping Lu, Haohao Zhang, and Fang Bai

Cite This: *ACS Omega* 2022, 7, 9254−9266

Read Online

ACCESS | Metrics & More | Article Recommendations | Supporting Information

ABSTRACT: Trichlorosilane (TCS) is a crucial intermediate product in the polysilicon manufacturing process, and its purification consumes a significant amount of energy. The design and control of the TCS heat integration pressure-swing distillation (HIPSD) process was investigated using Aspen Plus V8.4 and Aspen dynamics in this study. Three partial processes and one full HIPSD process were investigated by adjusting the operating conditions and rationally configuring the material flow. Compared with the conventional distillation process, the partial and full HIPSD can reduce total annual cost by 15.75 and 27.39%, respectively. The aforementioned process was controlled robustly by adding the ratio of reboiler heat duty to feed (Q_R/F) feedforward control structure and the ratio of recycle to feed (F_{REC}/F) control structure. In addition, the performance of the control structure was evaluated by introducing ±10% disturbances of the feed flowrate and composition. To compare the performance of the control structure, the integral squared error value is combined with the dynamic response curve. The full HIPSD scheme can resist ±10% disturbances of flow and composition with the best economic performance. This study has certain reference significance for the distillation process and control strategy design of TCS in the polysilicon manufacturing process.

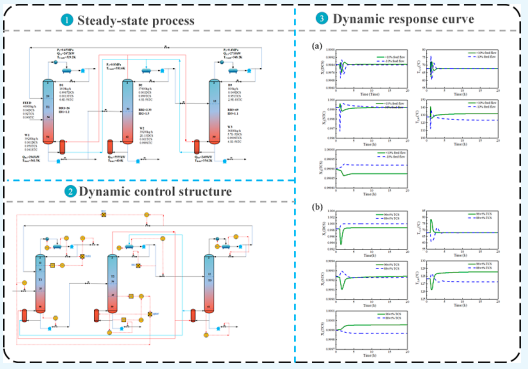

1. INTRODUCTION

Polysilicon is the main raw material for solar cells and semiconductor equipment, and it plays an extremely important role in the development of the photovoltaic industry.[1,2] In recent years, as many countries have successively established carbon neutrality goals and guided economic green and low-carbon development, the demand for polysilicon has grown rapidly.[3−5] The improved Siemens process is the mainstream polysilicon production process in the world today.[6] The processes include trichlorosilane (TCS) synthesis, TCS distillation and purification, TCS decomposition, and hydrogen reduction in the chemical vapor deposition reactor.[7] TCS purity has a direct impact on polysilicon quality; hence, TCS purification is an important stage in the polysilicon manufacturing process.

Among all separation technologies, distillation is currently the most widely used mixture separation technology in industrial processes, and distillation consumes about 95% of the total energy in the chemical separation industry.[8] Despite its high energy consumption, distillation remains the preferred method due to its processing advantages in operation and control, as well as a wealth of theoretical and practical knowledge. There are many advanced process intensification and integration techniques that can overcome the shortcomings of energy-intensive distillation, such as thermally coupled distillation,[9−12] dividing-wall columns (DWCs),[13−16] side-stream distillation,[17−20] or heat-integrated distillation.[21−25]

Díez et al.[26] studied the heat pump (HP)-assisted distillation to obtain TCS with a purity higher than 99.999% mol fraction. The double HP-assisted system reduced the total annual cost (TAC) by 29% compared with the conventional two-column distillation process and reached the goal of saving energy consumption. Wang et al. studied the use of Kaibel Dividing Wall Column (Kaibel DWC) to improve the performance of the TCS purification process.[27] The results showed that the Kaibel DWC saved 26.43% on energy and had a lower equipment cost when compared to the conventional configuration. Qie et al.[28] compared a series of energy-saving technologies to purify TCS, including the conventional process, the conventional process coupled with HP, the multi-effect distillation process, and the DWC process. The results demonstrated that the conventional process coupled with the HP technology has advantages over other distillation schemes for TCS purification in terms of the energy saving and economic effects. Huang et al.[29] developed heat integration pressure-swing distillation (HIPSD) for high-purity TCS to achieve heat integration and process optimization. The results

Received: October 23, 2021
Accepted: January 21, 2022
Published: March 9, 2022

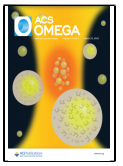

https://doi.org/10.1021/acsomega.1c05943
ACS Omega 2022, 7, 9254−9266

show that in the three-column high-purity TCS HIPSD process, the primary yield of TCS is 92%, and the theoretical energy savings is 66.7%.

Although heat integration distillation reduces energy consumption and improves efficiency, it is more complex than conventional distillation processes, making operability and controllability more difficult. The dynamic control of the heat integration distillation process is extensively investigated in many articles.[30−33] Liang et al.[34] reviewed the research development of pressure-swing distillation (PSD) by studying thermodynamic analysis, quantitative structure property relationship, process design, process intensification, and dynamic control. Cao et al.[33] compared the economy and dynamic controllability between extractive distillation and PSD of the azeotrope system. The investigation shows PSD is easier to control. Luyben[35,36] presented in detail the dynamic control of the partially HIPSD and full HIPSD for separating a tetrahydrofuran and water azeotrope and suggested some control schemes of the PSD for separating a maximum-boiling azeotropic mixture of methanol/trimethoxysilane. Li et al.[37] explored an improved control structure of pressure-swing heat integration reactive distillation for the hydrolysis of methyl acetate. The improved control structure can keep the system running smoothly and effectively handle large feed flow disturbances. However, very little study has been carried out on the dynamic control of high-purity chemical distillation, let alone the TCS distillation process. A robust and stable control system is essential to ensure high purity and safe operation.

In this manuscript, the design and parameter optimization of the HIPSD process with different heat integrations were studied. The sequential iteration method is used to achieve the optimal design parameters with the purpose of minimizing the TAC. For different TCS distillation schemes, corresponding control strategies are established to deal with the disturbances caused by changes in the feed flowrate and composition. Then, the value of the integral squared error (ISE) and the dynamic response curve as the standard were selected for evaluating the stability of the system.

2. STEADY-STATE SIMULATION

The accuracy of the simulation results mainly depends on the thermodynamic model used in simulation. In this work, the deviations between the NRTL, PENG-ROB, and RK-SOAVE thermodynamic model were compared according to the vapor−liquid equilibrium data reported by Zanta and Laskafeld;[38] the NRTL thermodynamic model resulted in the smallest deviation (Tables S1). The comparison between experimental and predicted data is shown in Figure 1 to validate the reliability of the thermodynamic model. Therefore, the NRTL thermodynamic method is reliable and can be used for subsequent simulations. Table 1 shows the binary interaction parameters used.

2.1. Conventional Distillation Process. Software Aspen Plus V8.4 were used to simulate the TCS distillation steady-state processes. Figure 2 show the flowsheet of the CD process. The feed flowrate is 40,000 kg/h with the compositions of 92.0 wt % TCS 4.0 wt % DCS and 4.0 wt % STC, which comes from actual industrial production.

First, the raw materials enter the light-removing column T1, product DCS (99.87 wt %) is taken out in the top (D1) of column T1. The bottom stream (95.8 wt % TCS) of column T1 is fed into heavy-removing column T2. Product STC (99.90 wt %) is removed out in the bottoms (B2) of column T2. The distillate stream (99.9 wt % TCS) of column T2 is fed into column T3 to further purify, and product TCS (99.99 wt %) is removed out in the bottom (B3) of column T3. Another end is the recycle stream (89.70 wt % TCS) fed into column T1.

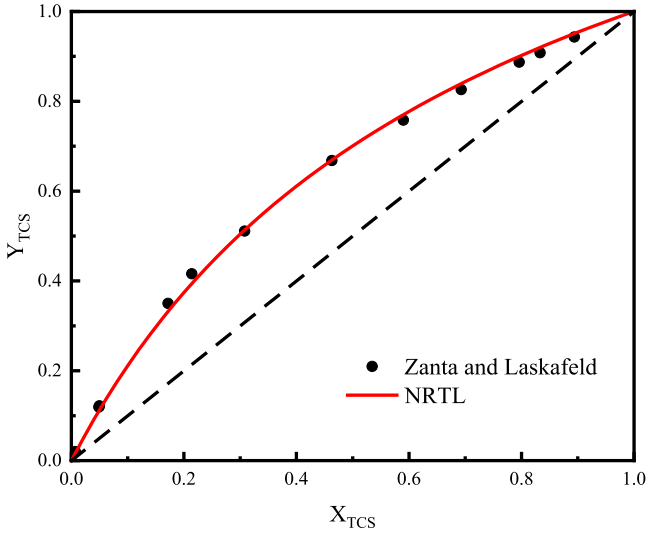

Figure 1. Pseudo-binary $Y-X$ diagram for $SiCl_3$ (1)-$SiCl_4$ (2) system at P = 0.987 bar, compared to the experimental data reported by Zanta and Laskafeld reproduced from ref 38. Reprinted with permission from Nelson, W. M.; Naidoo, P.; Ramjugernath, D. Phase equilibrium data for potentially hazardous binary mixtures involving dichlorosilane, trichlorosilane and silicon-tetrachloride. *J. Chem. Thermodyn.* **2015,** *91,* 420−426. Copyright 2015 Elsevier.

Table 1. Binary Interaction Parameters

parameter	DCS(i) + TCS(j)	DCS(i) + STC(j)	TCS(i) + STC(j)
A_{ij}	3.7408	2.7286	0.1118
A_{ji}	−0.1731	1.6205	0.2302
B_{ij}	−1152.52	0	−42.8361
B_{ji}	−36.3936	0	0.2446
C_{ij}	**0.3**	**0.3**	**0.3**

The operating pressure of the columns is determined based on the reflux temperature being sufficient to use cooling water (310 K) as cold utility. The appropriate pressures for T1, T2, and T3 are 0.45, 0.2, and 0.3 MPa, respectively. The optimal design parameters were determined with the minimum TAC as the objective function. Table S2 shows the economic basis for TAC calculation. In this table, the equipment calculation formula references to a study by Douglas,[39] and the utility price references to a study by Turton et al.[40] The equipment costs mainly include columns and heat exchangers, and other equipment such as pumps, valves, and vessels are ignored because their costs are much lower than the costs of columns and heat exchangers. In addition, the annual operating time was set to 8000 h, and the equipment payback period was set to 3 years.

The sequential iteration method[17] was used in the parameter optimization process, as shown in Figure 3. The parameters expected to be optimized include the number of stages in the T1, T2, and T3 columns (N_{T1}, N_{T2}, and N_{T3}), the feed locations (N_{F1}, N_{F2}, and N_{F3}), the recycle stream flowrate (F_{REC}), and the recycle location (N_{REC}). The "Design Spec/Vary" feature in Aspen Plus was used to ensure product specifications by adjusting reflux ratios (RR_1, RR_2, and RR_3).

https://doi.org/10.1021/acsomega.1c05943
ACS Omega 2022, 7, 9254−9266

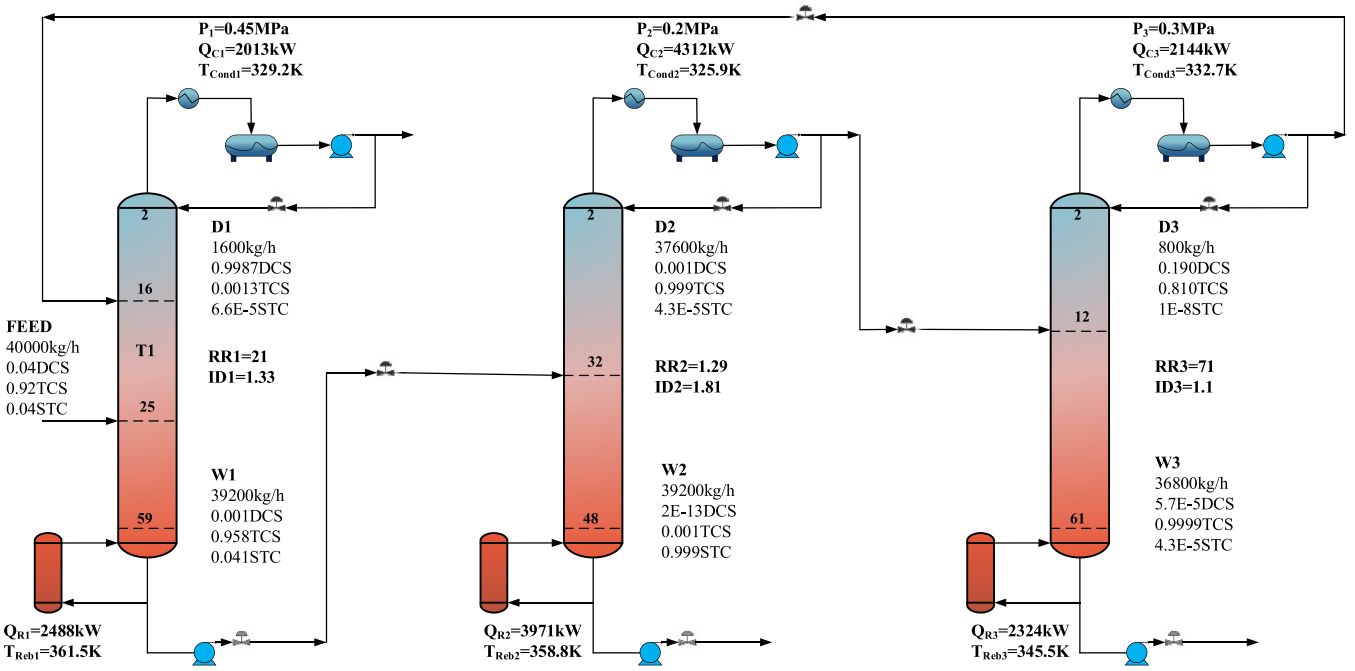

Figure 2. Flowsheet of the CD process.

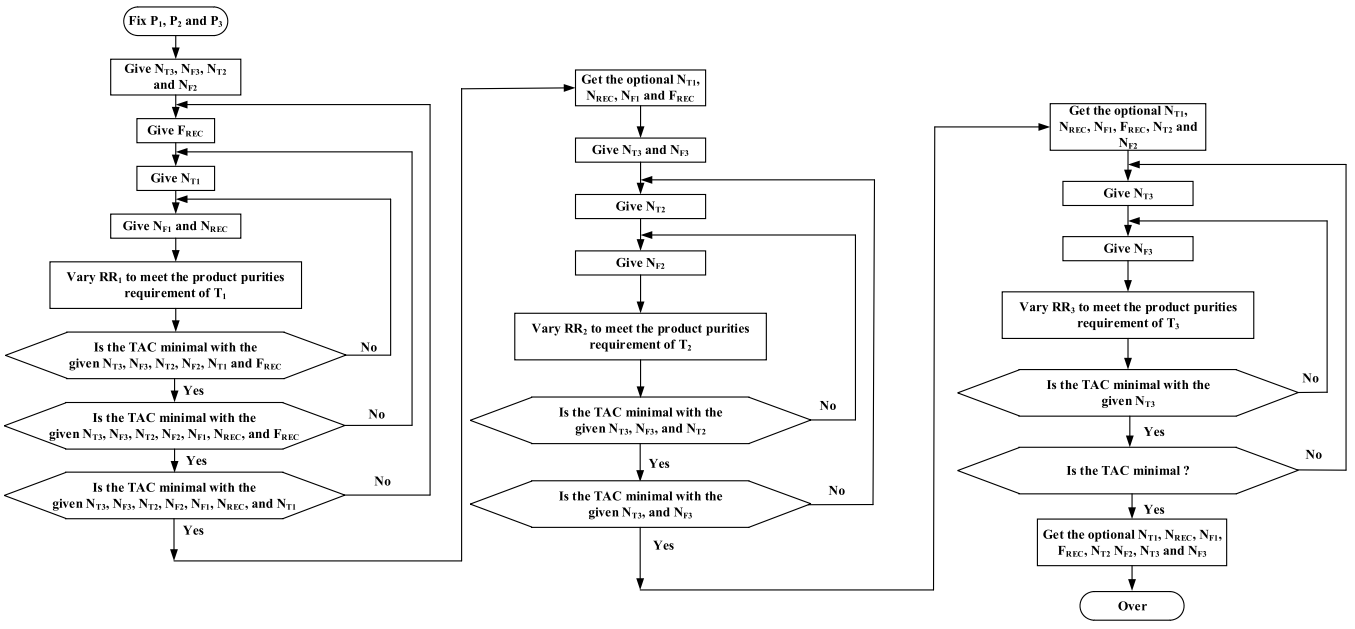

Figure 3. Sequential iterative optimization process of the separation process.

Finally, the minimum TAC is obtained through continuous iteration. Figure S1 shows the changes in TAC with the variables of the CD process. The optimized information of streams (D1, D2, and D3; B1, B2, and B3), columns (T1, T2, and T3), and operating parameters (pressure, temperature, and heat duty) are shown in Figure 2.

2.2. PSHID with Partial Heat Integration. The PSHID process involves heat transfer from the condenser of the high-pressure column (HPC) to the reboiler of the low-pressure column (LPC). The energy consumption of the condenser and reboiler of each column in the CD process is observed. The column with higher energy consumption is the heavy-removing column T2, and its energy consumption is basically the sum of the energy of the light-removing tower T1 and the secondary light-removing column T3. Therefore, it can be considered to appropriately change the operating pressure of each column and use the overhead stream of T2 to heat the reboiler of T1 and T3 to make full use of the heat.

There are three cases of the PSHID process with partial heat integration. (1) Heat integration between the condenser of T2 and the reboiler of T1, where the load of T2 condenser is greater than the load of T1 reboiler. As a result, an auxiliary condenser may be required to remove the excess heat. (2) Heat integration between T2 condenser and T3 reboiler, which is similar to the case 1, an auxiliary condenser is required. (3) Heat integration between T3 condenser and T1

https://doi.org/10.1021/acsomega.1c05943
ACS Omega 2022, 7, 9254−9266

Table 2. Parameters of Different Distillation Processes

variable	conventional distillation	PSHID with partial heat integration			PSHID with full heat integration
		case 1	case 2	case 3	
		Number of Stages			
N_{T1}	59	59	59	59	59
N_{T2}	49	60	60	56	60
N_{T3}	62	62	62	62	62
		Number of Feed/Recycle Locations			
N_{F1}/N_{REC}	25/16	25/16	25/16	25/16	25/16
N_{F2}	32	36	36	32	36
N_{F3}	12	12	12	12	12
		Reflux Ratio			
RR1	20.98	22.21	22.21	20.71	22.21
RR2	1.29	1.93	1.93	1.26	1.93
RR3	51.26	61.99	61.99	66.23	61.99
		Column Diameter			
ID_1 (m)	1.33	1.35	1.35	1.32	1.35
ID_2 (m)	1.81	1.82	1.82	1.78	1.82
ID_3 (m)	1.32	1.29	1.29	1.43	1.29
TAC ($/y)	2886623	2616706	2585632	2431875	2095988
optimization rate of TAC	0	−9.35%	−10.43%	−15.75%	−27.39%

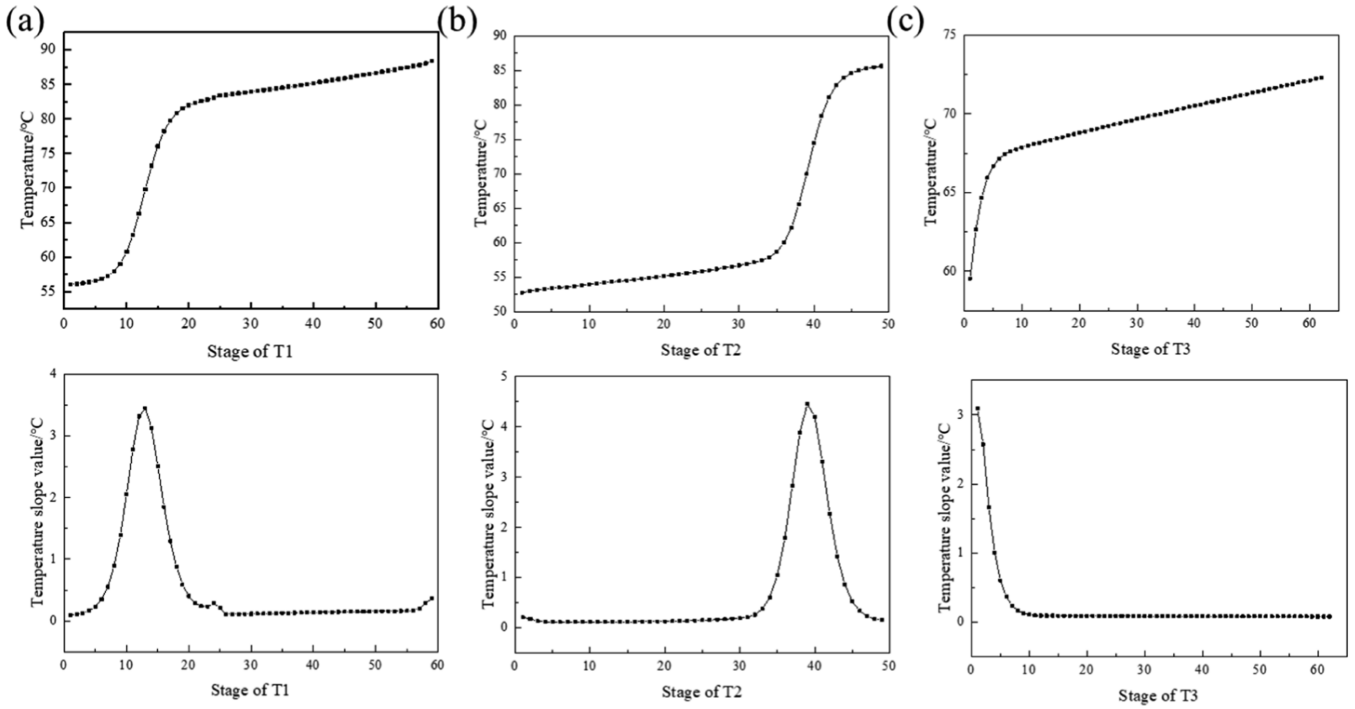

Figure 4. Temperature and temperature difference profiles: (a) T1, (b) T2, and (c) T3.

reboiler and their energy consumption are similar. In Aspen Plus V8.4, by adjusting the operating pressure in T3, the duty of T1 reboiler was equal to that of T3 condenser. Meanwhile, the pressure of T2 can be slightly reduced to reduce energy consumption.

In conclusion, the PSHID is implemented with partial thermal integration between the three columns. The detailed flowsheet of the partially heat integration PSHID process is shown in Figure S2.

2.3. PSHID with Full Heat Integration. For full heat integration, the condenser heat load of T2 exactly matches to the heat requirement of T1 and T3. The strategy of adjusting the T2 reflux ratio is a viable option for achieving this goal. Since the reboiler duty in the T2 (Q_{R2}) is the only heat input, a "neat" configuration can make the sum of reboiler duties of the T1 (Q_{R1}) and T3 (Q_{R3}) equal to the condenser duty of the T2 (Q_{C2}) using the "flowsheet design spec" function in Aspen Plus. In addition, Figure S3 shows the flowsheet of the PSHID process with full heat integration.

The important parameters of various processes are included in Table 2. As far as our simulation results are concerned, due to the use of the partial and full heat integration technology, compared with the CD configuration, the TAC can be reduced by 15.75 and 27.39%, respectively. However, the lack or increase in degrees of freedom will inevitably lead to more complicated and difficult dynamic control problems as energy

https://doi.org/10.1021/acsomega.1c05943
ACS Omega 2022, 7, 9254−9266

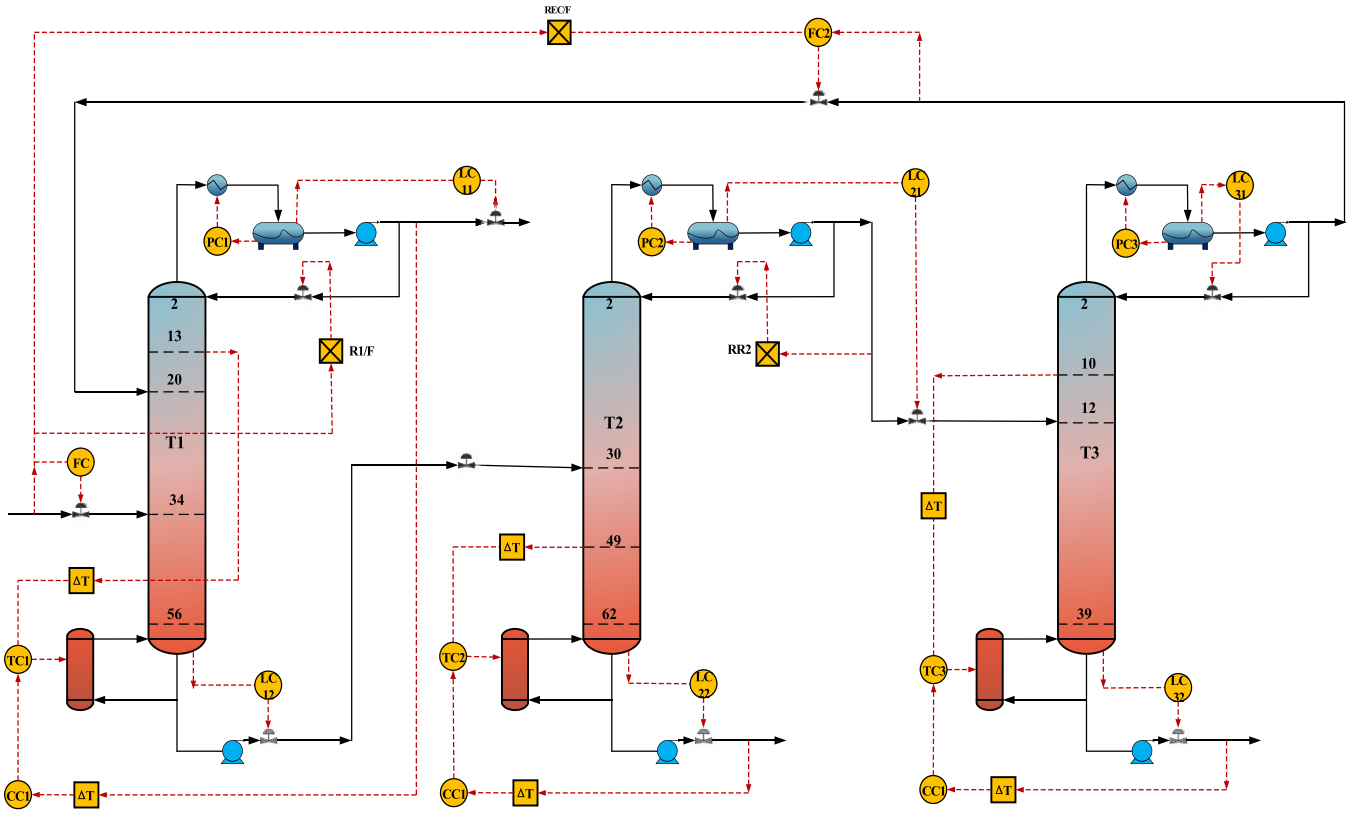

Figure 5. Control strategy CS1 for the conventional distillation process.

efficiency improves. To deal with the feed flowrate and feed composition disturbances, simple and feasible control structures of the three proposed alternative designs (CD, PSHID with partial and full heat integration) will be further developed and established.

3. DYNAMIC CONTROL

More important than steady-state design is research into the operability and dynamic controllability of high-efficiency separation configurations. By introducing the same feed flowrate and composition disturbance, the control structure of the above three alternative separation schemes is constructed and tested in this section.

The steady-state design flowsheet carried out in Aspen Plus V8.4 is exported to Aspen Plus Dynamics for dynamic simulation after dynamic parameters are specified. In this work, the tray pressure drop was 0.0068 atm, which ensures that the steady-state file can be exported to the dynamic state. The "Tray sizing" function in Aspen Plus V8.4 is used to determine the specifications of the column. The reflux drums, as well as the column bases, have been sized to allow for a 10 min residence time with the vessels half full. Furthermore, the reflux drums and column bases are roughly cylindrical, and the height is assumed to be double the diameter throughout the calculation.

3.1. Control of the CD Process. The determination of temperature-sensitive trays is an important step in the construction of control structures.[41] The temperature-sensitive trays were chosen using a slope criterion. Figure 4 shows the temperature and temperature difference profiles for the TCS CD process. The temperatures of stage 14 in T1 and stage 39 in T2 can be controlled by manipulating the corresponding reboiler duties. For T3, stage 20 is selected as the temperature-sensitive tray.

The control structure of the CD process is shown in Figure 5. The behavior of the controllers is as follows: (1) the pressures of both columns are controlled by manipulating the condenser duty. (2) The liquid level at the bottom of each column was controlled by the bottom material flowrate. (3) The liquid level of T1 and T2 reflux drums is controlled by manipulating the two distillate flows; the liquid level of T3 reflux drums is controlled by manipulating the reflux flow. (4) The heat duty of the reboiler of each column was used to control the temperature of the temperature-sensitive tray. (5) The set value of the temperature controller was based on the output of the product purity controller, forming a cascade control.

The usual tuning rules are applied to regular control loops with tuning constants of flow loops at K_c = 0.5 and τ_I = 0.3 min; level loops at K_c = 2.0 and τ_I = 9999 min; and pressure loops at K_c = 10.0 and τ_I = 20 min. Relay feedback testing and Tyreus−Luyben tuning rules are used to obtain the K_c and τ_I for temperature and composition controllers. A dead time of 1 min and 3 min was inserted into the temperature and composition control loop to allow for measurement delays.

The control performance of the control strategy was tested by adding flowrate and composition disturbance. For the feed flowrate disturbance, according to the actual fluctuation of the stream in the industrial production process, the feed flowrate was changed from 40,000 to 44,000 and 36,000 kg/h, respectively. When the composition disturbance was added, the feed composition changed to 0.02/0.96/0.02 (DCS/TCS/STC) and 0.06/0.88/0.06 (DCS/TCS/STC). The disturbance added in this work is relatively large for actual production and sufficient for theoretical research. Disturbance is added when

https://doi.org/10.1021/acsomega.1c05943
ACS Omega 2022, 7, 9254−9266

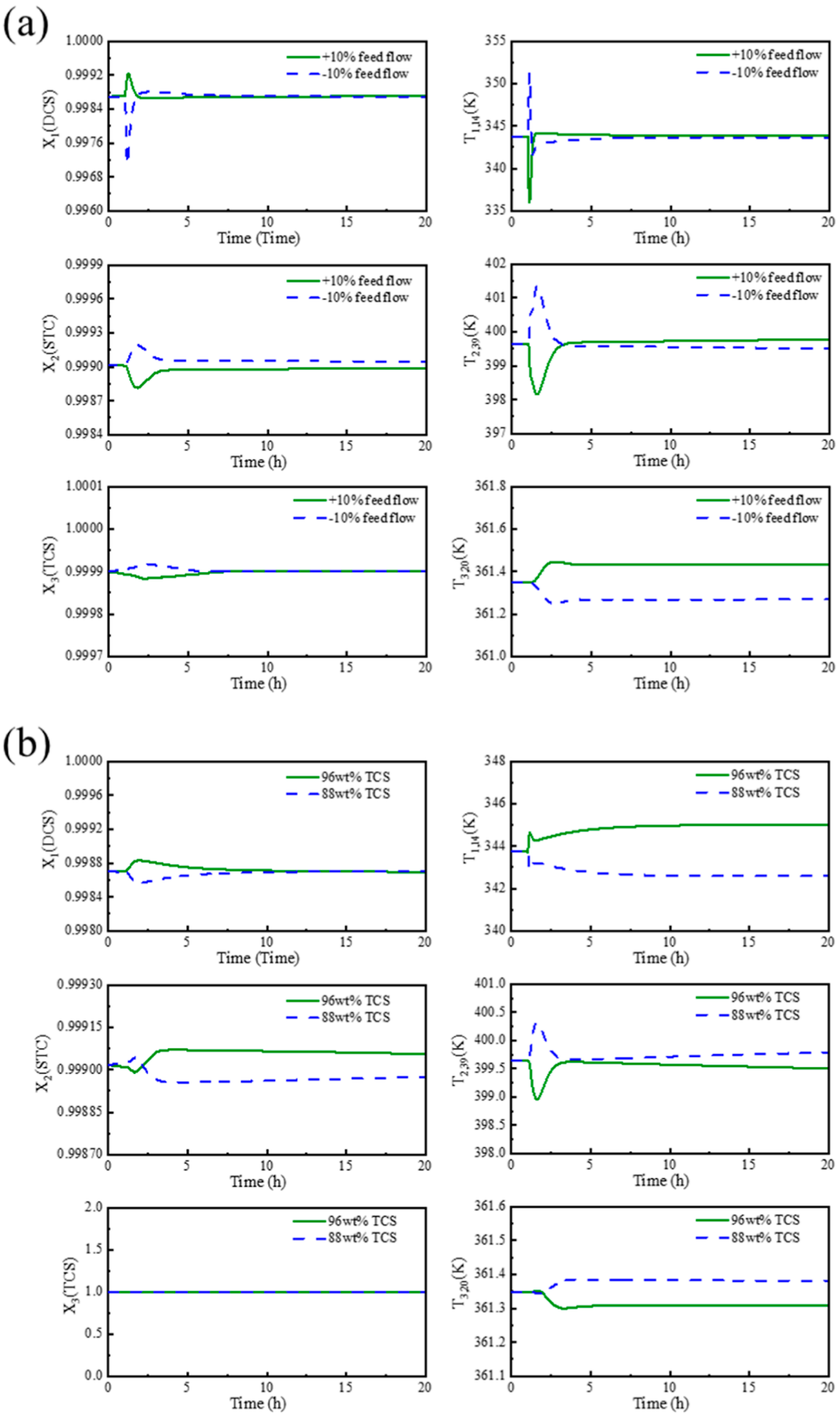

Figure 6. Closed-loop dynamic responses of the control strategy for CD: (a) feed flowrate disturbance and (b) feed composition disturbance.

https://doi.org/10.1021/acsomega.1c05943
ACS Omega 2022, 7, 9254−9266

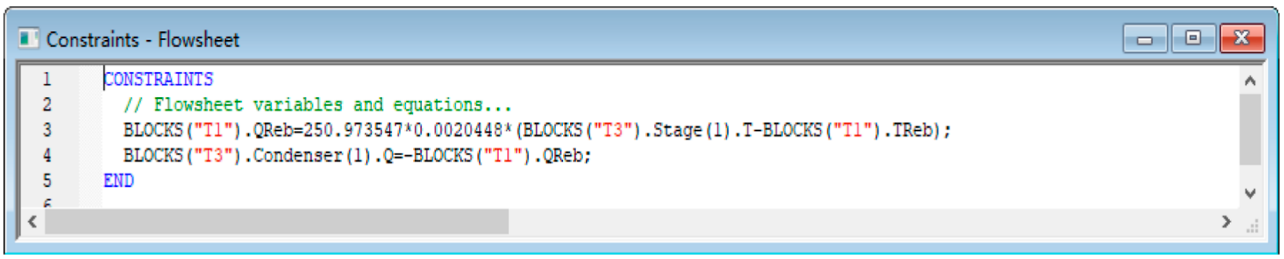

Figure 7. Equations for PSHID with partial heat integration.

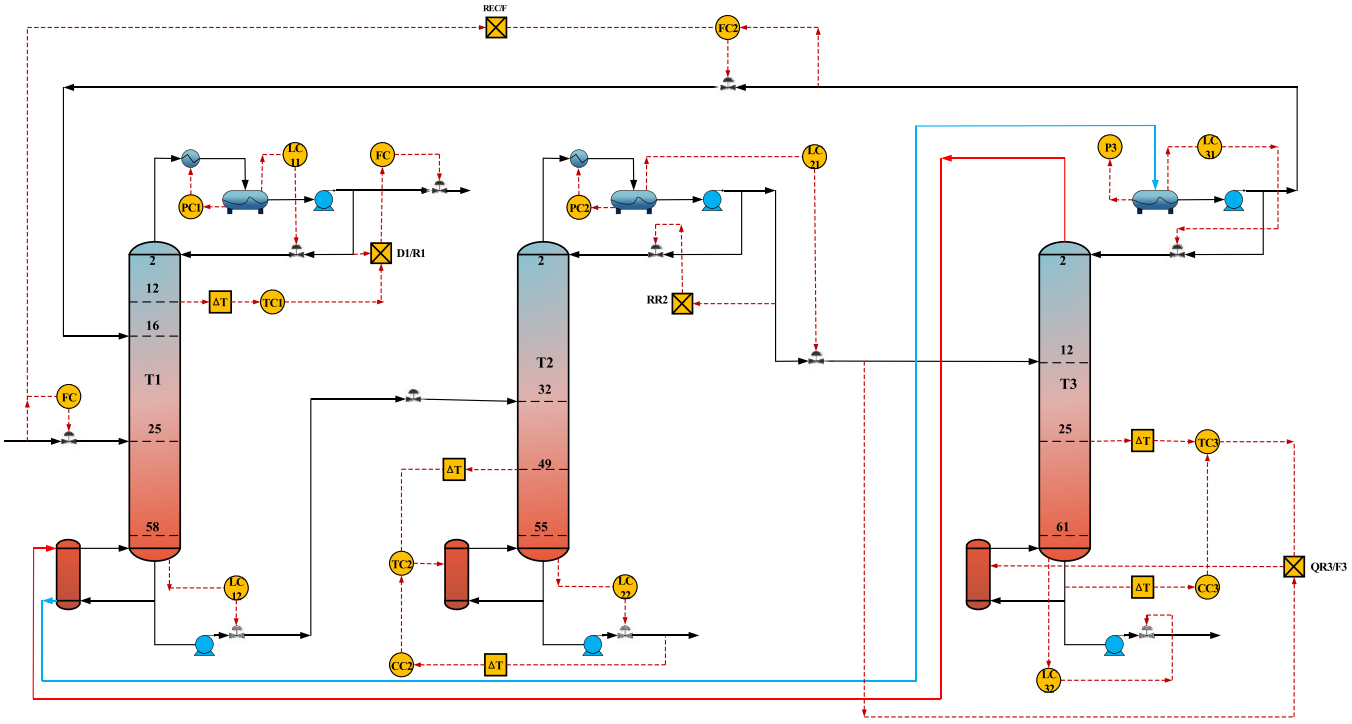

Figure 8. Control strategy CS2 for case 3 with partial heat integration.

the simulation runs for 1 h, and the entire test process will last for 20 h. Figure 6 shows the closed-loop dynamic responses of the control strategy for the conventional distillation process: (a) feed flowrate disturbance and (b) feed composition disturbance.

The purity of the key component TCS is stable in the system within 7 h after the feed flow is impeded, and the deviation of the stable value of other variables from the set value is small. The steady-state deviation increased slightly when the feed composition was changed. The purity of the key component TCS was not affected due to the strong effect of the temperature-composition cascade control.

3.2. Control of the PSHID with Partial Heat Integration. Table 2 shows that, among the three partial heat integration methods, case 3 has the smallest TAC. Therefore, a control strategy was designed based on the best economic process in case 3. In Aspen dynamics, the "Flowsheet equations" function was utilized to achieve partial heat integration. The flowsheet equations for the PSHID with partial heat integration is shown in Figure 7. For the calculation, the heat-transfer coefficient, heat-transfer area, T3 condenser temperature, and T1 reboiler temperature are all required. The heat-transfer coefficient is 0.0020448 GJ/(h m^2 K), the heat-transfer area is 250.97 m^2, and the temperature can be calculated using Aspen dynamics directly. The first equation is used to calculate the heat removal rate of T3 condenser. The second equation is used to calculate the heat input to T1 reboiler.

The control strategy for case 3 is shown in Figure 8. The partial heat integrated control strategy and the conventional distillation control strategy have some differences. This is due to the fact that the partial heat integration process reduces the degree of freedom of the control process. The main distinctions are as follows: (1) The "flowsheet equations" are used to calculate the load on the T3 condenser. As a result, T3 pressure will no longer be a free variable that can be controlled. (2) Because the flowsheet equations calculate the T1 reboiler load, the cascade control structure of T1 component-temperature control is modified to control the T1 distillation/reflux (D1/R1) ratio. (3) To improve the control structure's ability to handle feed disturbances, a new ratio control loop of reboiler duty to fresh flowrates ($Q_{R3}/F3$) is being considered. The temperature controller now controls the ratio of reboiler duty to fresh flowrates rather than the reboiler duty. All liquid level controllers have K_C of 2 and τ_I of 9999. The feed flow controller parameters remain unchanged; K_C is 0.5, and τ_I is 0.3. The temperature and component controller parameters are shown in Table S4.

https://doi.org/10.1021/acsomega.1c05943
ACS Omega 2022, 7, 9254−9266

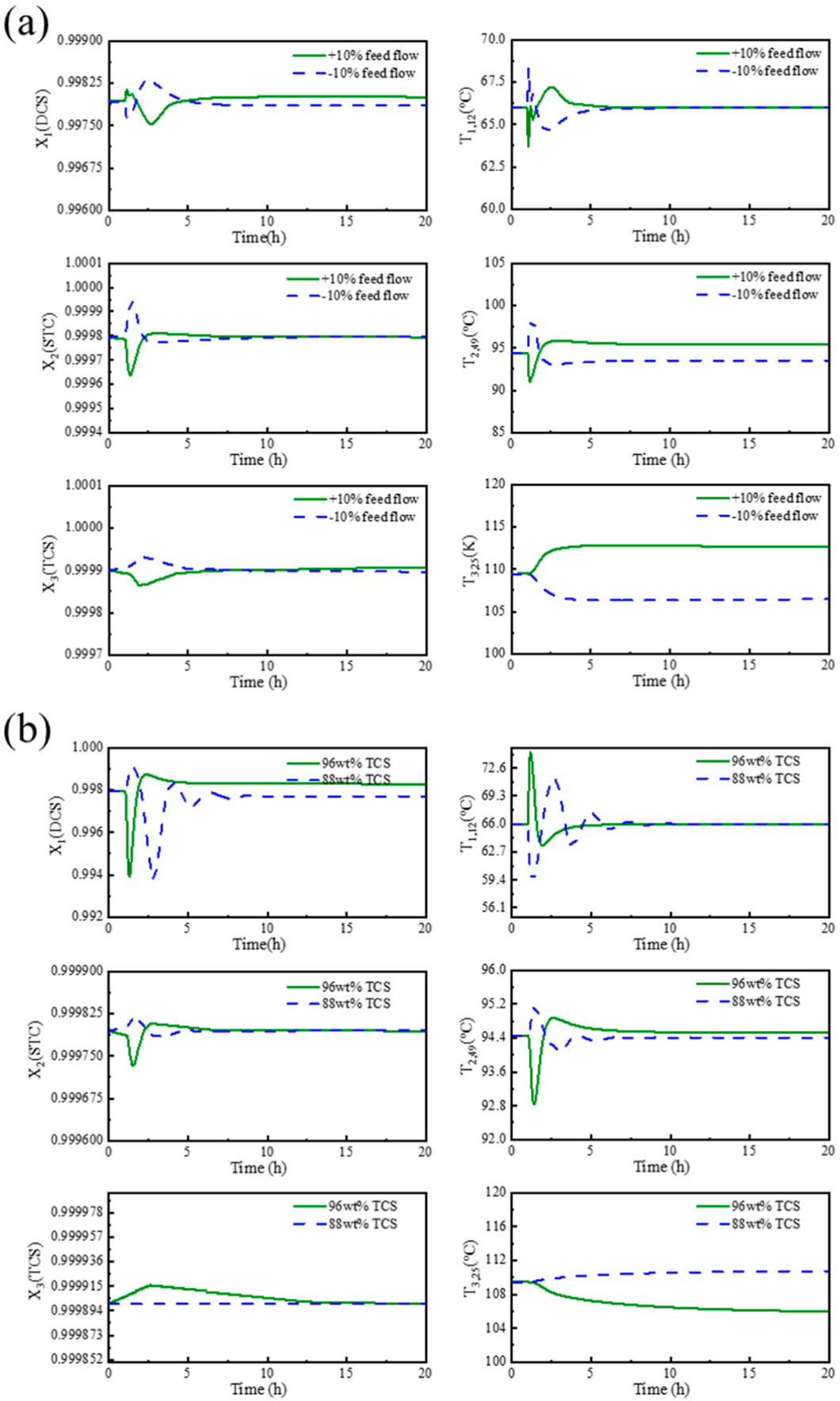

Figure 9. Closed-loop dynamic responses of the control strategy for case 3: (a) feed flowrate disturbance and (b) feed composition disturbance.

https://doi.org/10.1021/acsomega.1c05943
ACS Omega 2022, 7, 9254−9266

Constraints - Flowsheet

```
1   CONSTRAINTS
2     // Flowsheet variables and equations...
3     BLOCKS("T1").QReb=257.243424612984*0.0020448*(BLOCKS("T2").Stage(1).T-BLOCKS("T1").TReb);
4     BLOCKS("T3").QReb=154.633499262362*0.0020448*(BLOCKS("T2").Stage(1).T-BLOCKS("T3").TReb);
5     BLOCKS("T2").Condenser(1).Q=-BLOCKS("T3").QReb-BLOCKS("T1").QReb;
6   END
7
```

Figure 10. Equations for PSHID with full heat integration.

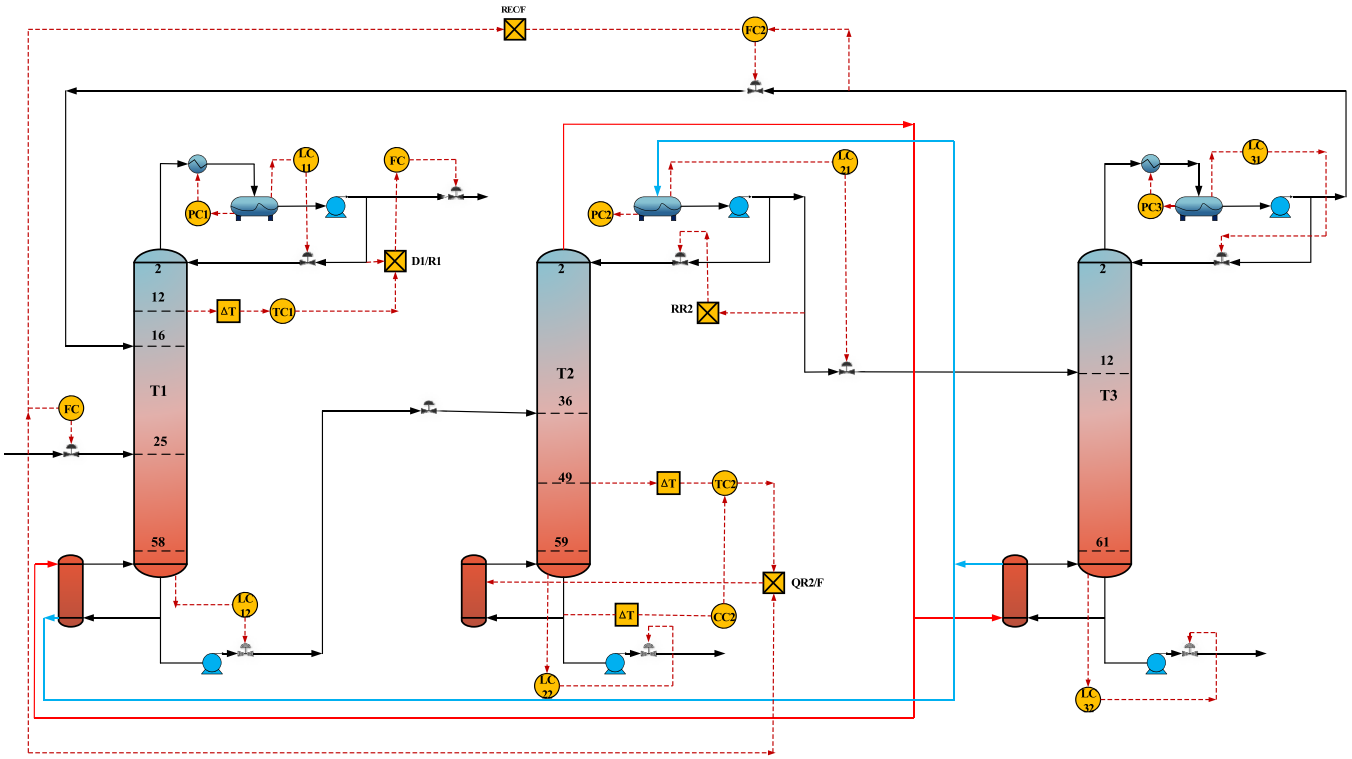

Figure 11. Control strategy CS3 of PSHID with full heat integration.

Then, the dynamic response of the control strategy is tested. The feed flowrate and composition disturbance were added, just like in conventional distillation. The disturbance was introduced during the first hour of the simulation, which lasted 20 h in total. The dynamic response of the control structure in case 3 is shown in Figure 9. Observing the control performances indicates that within 6 h, they are all returned to the value of the setpoint. With regard to the purity of three products, despite the disturbances in the feed composition, they are all kept at high purity. This demonstrates how well this control structure can resist disturbance.

3.3. Control of the PSHID with Full Heat Integration.

As mentioned in Section 2.3, since T2 undertakes the main separation task, its heat load is roughly equal to the sum of the heat loads of T1 and T3. In order to achieve full heat integration in this case, the steady-state parameters of the distillation column need to be adjusted and optimized with the goal of minimum TAC. The related design parameter results are shown in Table 2. The greater the degree of heat integration, the greater the economic advantages. At the same time, the degree of freedom of control of the distillation column decreases and the difficulty of control increases.

The flowsheet equations for the PSHID with full heat integration are shown in Figure 10. The first equation is to calculate the heat load of the reboiler for T1. The second equation is to calculate the heat load of the reboiler for T3. The third equation is to make the T2 condenser load equal to the sum of the T1 and T3 reboiler loads to achieve full heat integration. The heat exchange area is 257.23 and 154.63 m^2, respectively.

The PSHID control strategy with full heat integration is shown in Figure 11. The parameters of the liquid level and pressure control are the same as those in partial heat integration control structure. The parameters for temperature and composition control are shown in Table S5. It is worth mentioning that, compared with conventional distillation and partial heat integrated distillation, the control scheme of full heat integration has the following differences: (1) a feed-forward Q_{R2}/F structure is added to T2. The molar flowrate of the feed and the ratio of the reboiler duty to feed flow are the two input signals for this ratio control. (2) The control degree of freedom of T3 is reduced from two to zero. The recycle flowrate is set by the recycle-to-fresh feed flowrate (F_{REC}/F) ratio for column T3. Another degree of freedom is occupied by the heat integration between the columns.

https://doi.org/10.1021/acsomega.1c05943
ACS Omega 2022, 7, 9254−9266

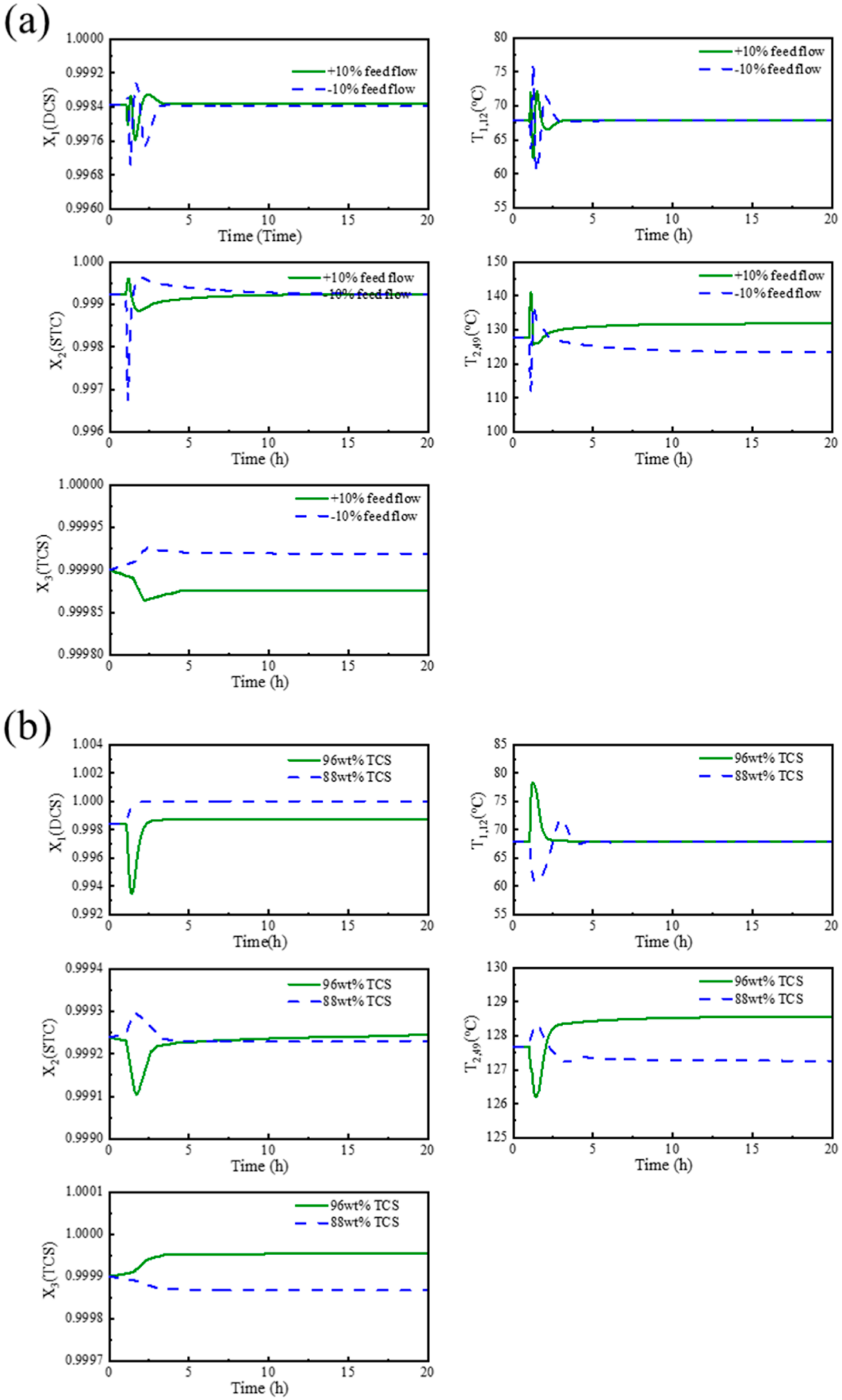

Figure 12. Closed-loop dynamic responses of the control strategy for PSHID with full heat integration: (a) feed flowrate disturbance and (b) feed composition disturbance.

https://doi.org/10.1021/acsomega.1c05943
ACS Omega 2022, 7, 9254−9266

Figure 12 gives the dynamic responses of the control strategy for PSHID with the full heat integration process: (a) feed flowrate disturbance and (b) feed composition disturbance, set up at 1 h. Both temperature control points can swiftly revert to their set points, as shown in the illustration. The purity of the product is maintained at a high level, and the purity fluctuation of each column is controlled within an acceptable range.

4. RESULTS AND DISCUSSION

The ISE is used to depict the dynamic performance of various control systems since it is an effective indicator that can reflect process variability.[42,43] The ISE value is calculated using eq 1.

$$\mathrm{ISE} = \int_{t_0}^{t} (y - y^{\mathrm{sp}})^2 \mathrm{d}t \tag{1}$$

In eq 1, t_0 represents the initial time of the dynamic simulation, t represents the final time, y^{sp} represents the set value of product purity, and y represents the actual purity of the product during operation. According to the definition of ISE, the smaller the value, the better the dynamic characteristics and the stronger the anti-interference ability.

Table 3 shows the ISE indicators of the three products in the face of different interferences for the three control structures.

Table 3. ISE Value for CS1, CS2, and CS3 Control Structures

		conventional distillation	PSHID with partial heat integration	PSHID with full heat integration
feed flowrates (+10%)	DCS	8.16×10^{-8}	2.45×10^{-7}	2.43×10^{-7}
	TCS	2.86×10^{-10}	1.62×10^{-9}	1.22×10^{-8}
	STC	6.16×10^{-8}	1.11×10^{-8}	2.14×10^{-7}
feed flowrates (−10%)	DCS	5.08×10^{-7}	2.58×10^{-7}	7.60×10^{-7}
	TCS	3.02×10^{-10}	1.43×10^{-9}	7.55×10^{-9}
	STC	4.98×10^{-8}	1.06×10^{-8}	1.12×10^{-6}
TCS:0.96	DCS	3.60×10^{-8}	7.63×10^{-6}	1.19×10^{-5}
	TCS	7.93×10^{-11}	6.02×10^{-10}	5.05×10^{-8}
	STC	3.89×10^{-8}	1.92×10^{-9}	1.32×10^{-8}
TCS:0.88	DCS	8.85×10^{-9}	1.31×10^{-5}	3.28×10^{-6}
	TCS	8.27×10^{-12}	7.23×10^{-11}	1.87×10^{-8}
	STC	1.21×10^{-8}	5.36×10^{-10}	2.88×10^{-9}

Comparing the ISE values of the three different processes, it is found that the ISE value of the CD process is the smallest, and the ISE value of PSHID with full heat integration process is the largest. This demonstrates that as the heat integration process improves, the controllability of the system deteriorates, which is consistent with our traditional thinking.

The time required for the three control strategies to restore product purity was compared to the design value in the face of feed flow disturbances. The conventional process, partial heat integration, and full heat integration control structures took 7, 7, and 4 h, respectively. From an economic point of view, the full heat integration process is economically optimal, and its TAC is reduced by 27.39% when compared to the CD process, as shown in Table 2. Combining the above two aspects, the full heat integration control structure has the best dynamic controllability and economy.

5. CONCLUSIONS

In this manuscript, the steady-state simulation and dynamic performance of the TCS distillation process are investigated under different heat integration processes. The sequential iteration method is used to obtain the best design parameters with the minimum TAC as the optimization goal. By adjusting the operating parameters and rationally arranging the material flow, three partial and one full PSHID processes were studied. The PSHID with full and partial heat integration process can reduce TAC by about 27.39% and 15.75%, as compared with the CD process, respectively. For the CD process, a robust cascade control strategy was developed, which can resist the flowrate and composition disturbances. It is worth mentioning that the snowball effect is eliminated or decreased by adding a F_{REC}/F ratio controller. Three partial heat integration processes have been developed by investigating heat integration between different distillation columns. In the TAC comparison, case 3 had the best economic performance and was chosen to design the control structure. After adding Q_{R}/F feedforward control to T3, it can better deal with disturbances. Full heat integration between the three columns is achieved by adjusting the reflux ratio and operating pressure of T2. Furthermore, after adding Q_{R}/F control, the full heat integration process achieves a stable control effect. Finally, by introducing the ISE evaluation index to analyze the anti-interference ability of the control structure, the study found that the ISE value of each control structure is very small, indicating that they can resist the disturbance caused by the feed flow and composition. The control strategy of full heat integration is the most economic and does not increase the difficulty of control when compared to other processes. This research has implications for the purification of TCS and the design of TCS control strategies in the polysilicon manufacturing process.

■ ASSOCIATED CONTENT

Supporting Information

The Supporting Information is available free of charge at https://pubs.acs.org/doi/10.1021/acsomega.1c05943.

TACs of CD under different parameters: stage number of T1, feed stage of T1, feed stage of recycle stream, stage number of T2, and feed stage of T2; flowsheet of the PSHID with partial heat integration: case 1, case 2, and case 3; flowsheet of the PSHID with full heat integration; deviation among three physical property methods (TCS-STC and VLE data); basis of economics; parameters of the temperature controllers and composition controllers in the CD process; parameters of the temperature controllers and composition controllers in the PSHID with partial heat integration; and parameters of the temperature controllers and composition controllers in the PSHID with full heat integration (PDF)

■ AUTHOR INFORMATION

Corresponding Author

Chao Hua − *Innovation Academy for Green Manufacture and Key Laboratory of Green Process and Engineering, Institute of Process Engineering, Chinese Academy of Sciences, Beijing 100190, PR China;* orcid.org/0000-0001-9747-4656; Email: huachao@ipe.ac.cn

https://doi.org/10.1021/acsomega.1c05943
ACS Omega 2022, 7, 9254−9266

Authors

Min Yin − *Innovation Academy for Green Manufacture and Key Laboratory of Green Process and Engineering, Institute of Process Engineering, Chinese Academy of Sciences, Beijing 100190, PR China; School of Chemical and Engineering, University of Chinese Academy of Sciences, Beijing 100190, PR China;* orcid.org/0000-0003-4857-5324

Ping Lu − *Innovation Academy for Green Manufacture and Key Laboratory of Green Process and Engineering, Institute of Process Engineering, Chinese Academy of Sciences, Beijing 100190, PR China*

Haohao Zhang − *Innovation Academy for Green Manufacture and Key Laboratory of Green Process and Engineering, Institute of Process Engineering, Chinese Academy of Sciences, Beijing 100190, PR China; School of Chemical and Engineering, University of Chinese Academy of Sciences, Beijing 100190, PR China*

Fang Bai − *Innovation Academy for Green Manufacture and Key Laboratory of Green Process and Engineering, Institute of Process Engineering, Chinese Academy of Sciences, Beijing 100190, PR China; School of Chemical and Engineering, University of Chinese Academy of Sciences, Beijing 100190, PR China*

Complete contact information is available at: https://pubs.acs.org/10.1021/acsomega.1c05943

Notes

The authors declare no competing financial interest.

■ ACKNOWLEDGMENTS

This work was supported by the National Key Research and Development Program of China (no. 2019YFC1907600) and by the Innovation Academy for Green Manufacture, Chinese Academy of Sciences (no. IAGM2020C08).

■ ABBREVIATIONS

CD, conventional distillation
CVD, chemical vapor deposition
DCS, dichlorosilane SiH_2Cl_2
TCS, trichlorosilane $SiHCl_3$
STC, silicon-tetrachloride $SiCl_4$
PSHID, pressure-swing heat integration distillation
TAC, total annual cost
K_C, gain of the controller
τ_I, integral time of the controller (min)
ISE, integral of squared error
y, actual purity of the product during operation
y^{sp}, set value of product purity
t_0, initial time of the dynamic simulation
t, final time of the dynamic simulation

■ REFERENCES

(1) Bódis, K.; Kougias, I.; Taylor, N.; Jäger-Waldau, A. Solar Photovoltaic Electricity Generation: A Lifeline for the European Coal Regions in Transition. *Sustainability* **2019**, *11*, 3703.

(2) Reese, M. O.; Glynn, S.; Kempe, M. D.; McGott, D. L.; Dabney, M. S.; Barnes, T. M.; Booth, S.; Feldman, D.; Haegel, N. M. Increasing Markets and Decreasing Package Weight for High-Specific-Power Photovoltaics. *Nat. Energy* **2018**, *3*, 1002−1012.

(3) Tozer, L.; Klenk, N. Discourses of Carbon Neutrality and Imaginaries of Urban Futures. *Energy Res. Social Sci.* **2018**, *35*, 174−181.

(4) Laine, J.; Heinonen, J.; Junnila, S. Pathways to Carbon-Neutral Cities Prior to a National Policy. *Sustainability* **2020**, *12*, 2445.

(5) Gnatowska, R.; Moryń-Kucharczyk, E. The Place of Photovoltaics in Poland's Energy Mix. *Energies* **2021**, *14*, 1471.

(6) Zhou, Y.-m.; Hou, Y.-q.; Nie, Z.-f.; Xie, G.; Ma, W.-h.; Dai, Y.-n.; Ramachandran, P. A. Thermodynamic Simulation of Polysilicon Production in Si-H-Cl System by Modified Siemens Process. *J. Chem. Eng. Jpn.* **2017**, *50*, 457−469.

(7) Dazhou, Y. *Siemens Process; Handbook of Photovoltaic Silicon*; Springer: Berlin, Heidelberg, 2018.

(8) Mahdi, T.; Ahmad, A.; Nasef, M. M.; Ripin, A. State-of-the-Art Technologies for Separation of Azeotropic Mixtures. *Sep. Purif. Rev.* **2014**, *44*, 308−330.

(9) Zhao, Y.; Ma, K.; Bai, W.; Du, D.; Zhu, Z.; Wang, Y.; Gao, J. Energy-saving thermally coupled ternary extractive distillation process by combining with mixed entrainer for separating ternary mixture containing bioethanol. *Energy* **2018**, *148*, 296−308.

(10) Zhang, Q.; Liu, Y.; Guo, T.; Xu, P.; Wang, Y. Comparison of the Improved Processes for Amyl Acetate Synthesis by Reactive Distillation in Different Operating Modes. *Asia-Pac. J. Chem. Eng.* **2019**, *14*, No. e2373.

(11) Yang, A.; Jin, S.; Shen, W.; Cui, P.; Chien, I.-L.; Ren, J. Investigation of Energy-Saving Azeotropic Dividing Wall Column to Achieve Cleaner Production via Heat Exchanger Network and Heat Pump Technique. *J. Cleaner Prod.* **2019**, *234*, 410−422.

(12) Ma, Z.; Yao, D.; Zhao, J.; Li, H.; Chen, Z.; Cui, P.; Zhu, Z.; Wang, L.; Wang, Y.; Ma, Y.; Gao, J. Efficient recovery of benzene and n-propanol from wastewater via vapor recompression assisted extractive distillation based on techno-economic and environmental analysis. *Process Saf. Environ. Prot.* **2021**, *148*, 462−472.

(13) Dejanović, I.; Matijašević, L.; Olujić, Ž. Dividing wall column-A breakthrough towards sustainable distilling. *Chem. Eng. Process.* **2010**, *49*, 559−580.

(14) Long, N. V. D.; Lee, M. Review of Retrofitting Distillation Columns Using Thermally Coupled Distillation Sequences and Dividing Wall Columns to Improve Energy Efficiency. *J. Chem. Eng. Jpn.* **2014**, *47*, 87−108.

(15) Feng, Z.; Shen, W.; Rangaiah, G. P.; Dong, L. Closed-Loop Identification and Model Predictive Control of Extractive Dividing-Wall Column. *Chem. Eng. Process.* **2019**, *142*, 107552.

(16) van Diggelen, R. C.; Kiss, A. A.; Heemink, A. W.; Research, E.-C. Comparison of Control Strategies for Dividing-Wall Columns. *Ind. Eng. Chem. Res.* **2010**, *49*, 288.

(17) Wang, Y.; Ma, K.; Yu, M.; Dai, Y.; Yuan, R.; Zhu, Z.; Gao, J. An improvement scheme for pressure-swing distillation with and without heat integration through an intermediate connection to achieve energy savings. *Comput. Chem. Eng.* **2018**, *119*, 439−449.

(18) Pan, Q.; Li, J.; Shang, X.; Ma, S.; Liu, J.; Sun, M.; Sun, L. Controllability, Energy-Efficiency, and Safety Comparisons of Different Control Schemes for Producing n-Butyl Acetate in a Reactive Dividing Wall Column. *Ind. Eng. Chem. Res.* **2019**, *58*, 9675−9689.

(19) Shi, T.; Chun, W.; Yang, A.; Su, Y.; Jin, S.; Ren, J.; Shen, W. Optimization and Control of Energy Saving Side-Stream Extractive Distillation with Heat Integration for Separating Ethyl Acetate-Ethanol Azeotrope. *Chem. Eng. Sci.* **2020**, *215*, 115373.

(20) Yang, J.; Hou, Z.; Dai, Y.; Ma, K.; Cui, P.; Wang, Y.; Zhu, Z.; Gao, J. Dynamic control analysis of interconnected pressure-swing distillation process with and without heat integration for separating azeotrope. *Chin. J. Chem. Eng.* **2021**, *29*, 67−76.

(21) Jana, A. K. Heat Integrated Distillation Operation. *Appl. Energy* **2010**, *87*, 1477−1494.

(22) Zhang, Q.; Liu, M.; Li, C.; Zeng, A. Heat-Integrated Pressure-Swing Distillation Process for Separation of the Maximum-Boiling Azeotrope Diethylamine and Methanol. *J. Taiwan Inst. Chem. Eng.* **2018**, *93*, 644−659.

(23) Zhang, Q.; Liu, M.; Li, C.; Zeng, A. Heat-Integrated Pressure-Swing Distillation Process for Separating the Minimum-Boiling Azeotrope Ethyl-Acetate And Ethanol. *Sep. Purif. Technol.* **2017**, *189*, 310−334.

(24) Wang, Y.; Zhang, Z.; Xu, D.; Liu, W.; Zhu, Z. Design and Control of Pressure-Swing Distillation for Azeotropes with Different Types of Boiling Behavior at Different Pressures. *J. Process Control* **2016**, *42*, 59−76.
(25) Shan, B.; Sun, D.; Zheng, Q.; Zhang, F.; Wang, Y.; Zhu, Z. Dynamic control of the pressure-swing distillation process for THF/ethanol/water separation with and without thermal integration. *Sep. Purif. Technol.* **2021**, *268*, 118686.
(26) Díez, E.; Rodríguez, A.; Gómez, J. M.; Olmos, M. Distillation Assisted Heat Pump in A Trichlorosilane Purification Process. *Chem. Eng. Process.* **2013**, *69*, 70−76.
(27) Wang, S.; He, Y.; Gao, Y.; Wang, Y.; Zhu, H. Simulation of Four-Product Dividing Wall Columns for the Separation of Trichlorosilane. *Chem. Ind. Eng.* **2018**, *35*, 72−79.
(28) Qie, S.-Y.; Pang, W.; Zhao, M.; Huang, Z. Application of Energy Saving Technology in Trichlorosilane Distillation Purification Process. *China Pet. Process. Petrochem. Technol.* **2019**, *21*, 94−102.
(29) Huang, G.; Shi, Z.; Wang, H. Energy Saving Technology Research on the Trichlorosilane Distillation in Polysilicon ProductionA wideband low power low phase noise dual-modulus prescaler. *Chem. Ind. Eng. Prog.* **2011**, *32*, 025011.
(30) Zhao, F.; Xu, Z.; Zhao, J.; Wang, J.; Hu, M.; Li, X.; Zhu, Z.; Cui, P.; Wang, Y.; Ma, Y. Process design and multi-objective optimization for separation of ternary mixtures with double azeotropes via integrated quasi-continuous pressure-swing batch distillation. *Sep. Purif. Technol.* **2021**, *276*, 119288.
(31) Luo, B.; Feng, H.; Sun, D.; Zhong, X. Control of fully heat-integrated pressure swing distillation for separating isobutyl alcohol and isobutyl acetate. *Chem. Eng. Process.* **2016**, *110*, 9−20.
(32) Li, X.; Yang, X.; Wang, S.; Yang, J.; Wang, L.; Zhu, Z.; Cui, P.; Wang, Y.; Gao, J. Separation of ternary mixture with double azeotropic system by a pressure-swing batch distillation integrated with quasi-continuous process. *Process Saf. Environ. Prot.* **2019**, *128*, 85−94.
(33) Cao, Y.; Hu, J.; Jia, H.; Bu, G.; Zhu, Z.; Wang, Y. Comparison of pressure-swing distillation and extractive distillation with varied-diameter column in economics and dynamic control. *J. Process Control* **2017**, *49*, 9−25.
(34) Liang, S.; Cao, Y.; Liu, X.; Li, X.; Zhao, Y.; Wang, Y.; Wang, Y. Insight into pressure-swing distillation from azeotropic phenomenon to dynamic control. *Chem. Eng. Res. Des.* **2017**, *117*, 318−335.
(35) Luyben, W. L. Design and Control of a Fully Heat-Integrated Pressure-Swing Azeotropic Distillation System. *Ind. Eng. Chem. Res.* **2008**, *47*, 2681−2695.
(36) Luyben, W. L. Control of a Heat-Integrated Pressure-Swing Distillation Process for the Separation of a Maximum-Boiling Azeotrope. *Ind. Eng. Chem. Res.* **2014**, *53*, 18042−18053.
(37) Li, L.; Sun, L.; Wang, J.; Zhai, J.; Liu, Y.; Zhong, W.; Tian, Y. Design and Control of Different Pressure Heatly Coupled Reactive Distillation for Methyl Acetate Hydrolysis. *Ind. Eng. Chem. Res.* **2015**, *54*, 12342−12353.
(38) Nelson, W. M.; Naidoo, P.; Ramjugernath, D. Phase equilibrium data for potentially hazardous binary mixtures involving dichlorosilane, trichlorosilane and silicon-tetrachloride. *J. Chem. Thermodyn.* **2015**, *91*, 420−426.
(39) Douglas, J. M. *Conceptual Design of Chemical Processes*; McGraw-Hill: New York, 1988; Vol. *1110*.
(40) Turton, R. *Analysis, Synthesis and Design of Chemical Processes*; Pearson Edition, 2012.
(41) Luyben, W. L. *Distillation Design and Control Using Aspen Simulation*; Wiley: New York, 2013.
(42) Dai, Y.; Xu, Y.; Wang, S.; Li, S.; Wang, Y.; Gao, J. Dynamics of Hybrid Processes with Mixed Solvent for Recovering Propylene Glycol Methyl Ether from Wastewater with Different Control Structures. *Sep. Purif. Technol.* **2019**, *229*, 115815.
(43) Zhu, Z.; Li, S.; Dai, Y.; Yang, X.; Wang, Y.; Gao, J. Control of a Pressure-Swing Distillation Process for Benzene/Isopropanol/Water Separation with and without Heat Integration. *Sep. Purif. Technol.* **2020**, *236*, 116311.

https://doi.org/10.1021/acsomega.1c05943
ACS Omega 2022, 7, 9254−9266